THE JOURNAL OF BIOLOGICAL CHEMISTRY VOL. 285, NO. 12, pp. 8695–8702, March 19, 2010

MD-2-mediated Ionic Interactions between Lipid A and TLR4 Are Essential for Receptor Activation*[S]

Received for publication, October 12, 2009, and in revised form, December 11, 2009 Published, JBC Papers in Press, December 15, 2009, DOI 10.1074/jbc.M109.075127

Jianmin Meng, Egil Lien[1,2], and Douglas T. Golenbock[1,3]

From the Division of Infectious Diseases and Immunology, University of Massachusetts Medical School, Worcester, Massachusetts 01605

Lipopolysaccharide (LPS) activates innate immune responses through TLR4·MD-2. LPS binds to the MD-2 hydrophobic pocket and bridges the dimerization of two TLR4·MD-2 complexes to activate intracellular signaling. However, exactly how lipid A, the endotoxic moiety of LPS, activates myeloid lineage cells remains unknown. Lipid IV_A, a tetra-acylated lipid A precursor, has been used widely as a model for lipid A activation. For unknown reasons, lipid IV_A activates proinflammatory responses in rodent cells but inhibits the activity of LPS in human cells. Using stable TLR4-expressing cell lines and purified monomeric MD-2, as well as MD-2-deficient bone marrow-derived macrophages, we found that both mouse TLR4 and mouse MD-2 are required for lipid IV_A activation. Computational studies suggested that unique ionic interactions exist between lipid IV_A and TLR4 at the dimerization interface in the mouse complex only. The negatively charged 4′-phosphate on lipid IV_A interacts with two positively charged residues on the opposing mouse, but not human, TLR4 (Lys^{367} and Arg^{434}) at the dimerization interface. When replaced with their negatively charged human counterparts Glu^{369} and Gln^{436}, mouse TLR4 was no longer responsive to lipid IV_A. In contrast, human TLR4 gained lipid IV_A responsiveness when ionic interactions were enabled by charge reversal at the dimerization interface, defining the basis of lipid IV_A species specificity. Thus, using lipid IV_A as a selective lipid A agonist, we successfully decoupled and coupled two sequential events required for intracellular signaling: receptor engagement and dimerization, underscoring the functional role of ionic interactions in receptor activation.

Innate immunity is the first line of defense against exogenous pathogens. Activation of the innate immune system produces inflammatory cytokines such as tumor necrosis factor α and interleukin-1β, both of which help prevent infection and enhance the adaptive immune response (1). The effect of these cytokines can become detrimental when they are produced in abundance, resulting in sepsis syndrome. Indeed, Gram-negative septic shock still has high mortality (~20%) and remains a leading cause of death in noncoronary intensive care units in the United States (2, 3).

During Gram-negative bacterial infection, lipopolysaccharide (LPS),[4] the major component of the bacterial outer membrane, activates the innate immune response through the Toll-like receptor 4 (TLR4) and MD-2 complex. The active component of LPS is lipid A, a partially conserved glycolipid that anchors LPS into the outer membrane of Gram-negative bacteria. Stimulatory lipid As, such as *Escherichia coli* lipid A, usually have 6–8 acyl chains covalently linked to the diglucosamine bis-phosphorylated backbone. The phosphate groups at the 1,4′-position are essential for the agonist activity of lipid A, because monophosphorylated lipid A is greatly reduced in its proinflammatory activity (4). In addition, both the number and the length of the acyl chains are essential for the full agonist activity of lipid A (5–7). In fact, the production of a hypoacylated lipid A and the resulting evasion of innate immunity may be associated with virulence in pathogens such as *Yersinia pestis* (8). *E. coli* hexa-acylated lipid A acts as a pan-agonist for all mammalian cells that express a complete LPS receptor complex. The precursor of *E. coli* lipid A, tetra-acylated lipid IV_A (9), is only an agonist for some species of mammals (10).

Although commonly referred to as the LPS receptor, TLR4 does not directly bind LPS or any other LPS analog with high avidity. Instead, MD-2, a 25-kDa co-receptor that physically associates with TLR4 directly binds the lipid A moiety of LPS (or its analogs) through the central hydrophobic pocket (11–13). This hydrophobic pocket can accommodate up to five acyl chains. In contrast to commonly held notions that the MD-2 pocket would expand to accommodate additional acyl chains from stimulatory lipid A, the resolution of a co-crystal structure of human TLR4 (hTLR4), human MD-2 (hMD-2), and LPS (12) revealed that the sixth acyl chain of LPS is excluded from the hydrophobic pocket and present on MD-2 surface. Both hMD-2 and hTLR4 undergo "induced fit" conformational changes to allow dimerization to occur (12).

Although an LPS antagonist in human cells, lipid IV_A is an LPS mimetic when tested with mouse cells (14, 15). Several studies have been dedicated to understanding the molecular determinants of this species specificity. The results of these studies, however, are contradictory. Our group (16), as well as that of Beutler and co-workers (17), proposed that TLR4 is responsible for the species specificity of lipid IV_A. Yet, based on

* This work was supported, in whole or in part, by National Institutes of Health Grants GM54060 (to D. T. G.) and AI057588 (to E. L.).

[S] The on-line version of this article (available at http://www.jbc.org) contains supplemental Table S1 and Figs. S1–S8.

[1] Both authors contributed equally to this work.

[2] To whom correspondence may be addressed. Tel.: 508-856-5865; Fax: 508-856-5463; E-mail: egil.lien@umassmed.edu.

[3] To whom correspondence may be addressed. Tel.: 508-856-5980; Fax: 508-856-5463; E-mail: douglas.golenbock@umassmed.edu.

[4] The abbreviations used are: LPS, lipopolysaccharide; TLR, Toll-like receptor; h, human; BMDM, bone marrow-derived macrophage; DMEM, Dulbecco's modified Eagle's medium; m, mouse.

similar approaches, Miyake and co-workers (14) and Miller and co-workers (18) reported that MD-2 is responsible for the species-specific responses to lipid IV_A. A full interpretation of these studies was not possible because neither group could ever characterize the activity of human TLR4 with mouse MD-2 (mMD-2), probably because the latter protein is so poorly expressed in transfected cell lines. Using a slightly different system, *i.e.* comparing human *versus* equine genes, Bryant and co-workers (19) demonstrated that under defined conditions, MD-2 and TLR4 were both required for the species-specific activation of lipid IV_A, partially reconciling the contradiction between the two theories.

The present study addresses both the molecular determinants and the underlying mechanism of the species-specific activation of lipid IV_A in an attempt to truly understand the mystery of lipid IV_A activity and to extend our knowledge on the mechanism of lipid A activation. We found that both mouse TLR4 (mTLR4) and mMD-2 are required to confer LPS agonist activity to lipid IV_A, both in HEK293 cell lines that stably express hTLR4 or mTLR4 and in MD-2-deficient bone marrow-derived macrophages (BMDMs). We used computational docking and modeling to generate a dimeric mTLR4·mMD-2·lipid IV_A model to understand the underlying mechanism. We found that unique ionic interactions exist between lipid IV_A and TLR4 in the mouse complex only. When these ionic interactions were disrupted by mutagenesis, lipid IV_A responsiveness was severely impaired. In contrast, hTLR4 gained lipid IV_A responsiveness when ionic interactions were enabled by charge reversal at the dimerization interface, defining the basis for lipid IV_A species specificity. Because lipid A also lacks the core polysaccharide, ionic interactions between the phosphates on the lipid A diglucosamine backbone and the positively charged residues on TLR4 at the dimerization interface are likely to play a key role in receptor dimerization and activation. Thus, we provide direct evidence that ionic interactions between the lipids and TLR4, especially at the dimerization interface, play an essential role in triggering the dimerization and activation of the LPS receptor.

EXPERIMENTAL PROCEDURES

MD-2 Expression and Purification—The MD-2 constructs expressing hMD-2 and mMD-2 with a C-terminal protein A tag were gifts from Dr. Jie-Oh Lee (11). MD-2 proteins were expressed and purified as described earlier (11) (supplemental Fig. S1). The MD-2 concentrations were determined by UV absorbance at 280 nm using the extinction coefficients 18,490 and 14,650 liters·M^{-1}·cm^{-1} for hMD-2 and mMD-2, respectively (20).

Luciferase Assay—The HEK293/$mTLR4^{YFP}$ cell line was constructed as described earlier (21). The *E. coli* precursor, lipid IV_A, was synthesized as described (22). The synthetic compound, Eritoran, was a gift from the Eisai Research Institute (Andover, MA). LPS from *E. coli* strain O111:B4 (Sigma) was repurified by a repeat phenol chloroform extraction (23). HEK293/$hTLR4^{YFP}$ and HEK293/$mTLR4^{YFP}$ cells were plated in 96-well dishes at a density of 10,000 cells/well. The next day, the cells were transfected with a plasmid encoding for an NF-κB-luciferase gene and a control plasmid expressing *Renilla* luciferase. After overnight transfection, the supernatants were removed, and the cells were washed twice with phosphate-buffered saline and replenished with serum-free medium consisting of DMEM only. The cells were stimulated with 1) the indicated concentrations of LPS or lipid IV_A and 2) increasing concentrations of purified monomeric MD-2. After overnight stimulation, the supernatants were removed, and the luciferase activity was measured in cell lysates. *Renilla* luciferase was used for normalization.

The single, double, and triple mutants that swap surface charges between hTLR4 and mTLR4 at the dimerization interface were created by site-directed mutagenesis per the manufacturer's instructions (QuikChange). All of the mutations were verified by DNA sequencing (Genewiz, Inc., South Plainfield, NJ). The effects of these mutations on LPS and lipid IV_A signaling were tested in HEK293 cells by transient transfection. HEK293 cells were plated in 96-well plates at a density of 20,000 cells/well. The next day, the cells were transfected with 1) one of the $hTLR4^{YFP}$ or $mTLR4^{YFP}$ mutants (1 ng/well), 2) an NF-κB-luciferase plasmid (24), and 3) the *Renilla* luciferase plasmid. After overnight transfection, the supernatant was removed, and the cells were washed twice with phosphate-buffered saline and replenished with complete DMEM without serum. The cells were stimulated with the indicated concentrations of mMD-2 and LPS·lipid IV_A overnight prior to the determination of luciferase activity.

Tumor Necrosis Factor α Production—Mice deficient in MD-2 were a gift from Dr. Kensuke Miyake (25). BMDMs were differentiated in the presence of 20% L929 conditioned medium for 10 days. The cells were then plated in 96-well plates at a concentration of 50,000/well in complete DMEM supplemented with 10% fetal bovine serum. After attachment, the supernatants were removed, and the cells were washed four times with phosphate-buffered saline and replenished with serum-free DMEM. The cells were then stimulated with 1) a fixed concentration of lipid IV_A or LPS, 2) decreasing concentrations of purified, monomeric MD-2, and 3) 1 μg of CD14/ml (26). After overnight stimulation, the supernatants were saved, and the tumor necrosis factor α levels were measured by enzyme-linked immunosorbent assay.

Docking Procedure between Lipid IV_A and Human or Mouse MD-2—Docking studies were performed using AutoDock 4.0.1 (27, 28) with an AutoDockTool (29). The coordinates of lipid IV_A were subtracted from the co-crystal structure of hMD-2 and lipid IV_A (Protein Data Bank code 2E59) (13). To reduce expectation bias, the crystal structure of hMD-2 alone (Protein Data Bank code 2E56) (13) instead of from the hMD-2·lipid IV_A co-crystal structure (Protein Data Bank code 2E59) (13) was used for docking with lipid IV_A. The coordinates of mMD-2 were subtracted from the co-crystal structure of mMD-2 and mTLR4 (Protein Data Bank code 2Z64) (11). Both hMD-2 and mMD-2 were treated as rigid, and lipid IV_A was treated as flexible with 30 torsions during docking. The AutoGrid parameters are illustrated in detail in supplemental Table S1. Twenty structures were generated using genetic algorithm searches. A default protocol was applied, with an initial population of 150 randomly placed individuals, a maximum number of 2.5×10^6

energy evaluations, and a maximum number of 2.7×10^4 generations. A mutation rate of 0.02 and a cross-over rate of 0.8 were used.

Generation of a Dimeric mTLR4·mMD-2·Lipid IV$_A$ Complex—The coordinates of the docked mMD-2·lipid IV$_A$ complex were combined with the coordinates of mTLR4 extracted from the mTLR4/mMD-2 co-crystal structure (Protein Data Bank code 2Z64) (11) to generate a monomeric mTLR4·mMD-2·lipid IV$_A$ complex. Two copies of mTLR4·mMD-2·lipid IV$_A$ complexes were then aligned to the hTLR4·hMD-2·LPS co-crystal structure to generate a dimeric mTLR4·mMD-2·lipid IV$_A$ complex. The detailed alignment procedure is as follows: the mTLR4 sequences from the first mTLR4·mMD-2·lipid IV$_A$ complex were aligned to one hTLR4 sequences in the dimeric hTLR4·hMD-2·LPS co-crystal structure, and the mTLR4 sequences from the second mTLR4·mMD-2·lipid IV$_A$ complex were aligned to the other hTLR4 sequences in the co-crystal structure. The sequences of MD-2 and lipids were not used for the alignment. A dimeric mTLR4·mMD-2·lipid IV$_A$ complex was readily observed after the alignment.

RESULTS

The Full Mouse Receptor Complex, Consisting of Mouse TLR4 and Mouse MD-2, Is Required for the Full Agonist Activity of Lipid IV$_A$—To clarify the contradictions among different studies concerning lipid IV$_A$ species specificity, we developed stable cell line systems in which hTLR4 (21) or mTLR4 was stably expressed on the cell surface, allowing us to study each component separately and consistently. Monomeric soluble MD-2 of both human and mouse origin were purified (supplemental Fig. S1) and used as the source for MD-2.

We examined the inducible luciferase activity using an NF-κB reporter construct transiently transfected in HEK293 cells. Both HEK293/hTLR4^{YFP} (Fig. 1*a*) and HEK293/mTLR4^{YFP} cells (Fig. 1*b*) responded to LPS stimulation in an MD-2 dose-dependent manner, regardless of the species of MD-2 included. A peak response was observed at the MD-2 concentration of 40 ng/ml (1.3 nM), which likely reflects the optimal concentration of MD-2 to interact with TLR4 in HEK293 cells to activate intracellular signaling. Note that we have consistently observed that HEK293/hTLR4^{YFP} cells responded to LPS more vigorously with hMD-2 than with mMD-2, whereas HEK293/mTLR4^{YFP} cells responded to LPS similarly with hMD-2 and mMD-2.

When lipid IV$_A$ was used as the stimulant, HEK293/hTLR4^{YFP} cells did not respond to lipid IV$_A$ in the presence of either hMD-2 or mMD-2 at all of the tested concentrations (Fig. 1*a*); under these conditions, lipid IV$_A$ functioned as an LPS antagonist (supplemental Fig. S2). This is consistent with our previously reported data that lipid IV$_A$ acts as an antagonist in the presence of hTLR4 (16). In comparison, HEK293/mTLR4^{YFP} cells (Fig. 1*b*) responded to lipid IV$_A$ stimulation (*gray diamond* and *open square*) in a (mMD-2) dose-dependent manner that peaked at the mMD-2 concentration of 200 ng/ml (6.7 nM). This suggests that when both mMD-2 and mTLR4 are present, lipid IV$_A$ functions as an LPS agonist.

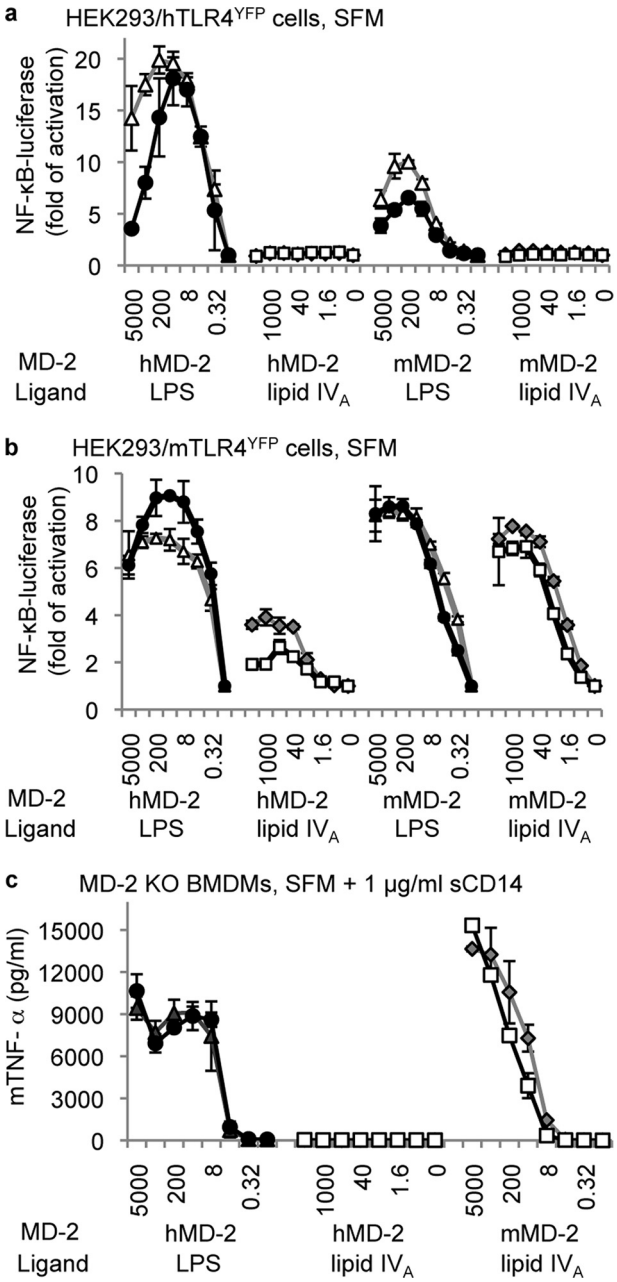

FIGURE 1. **Both mTLR4 and mMD-2 are required for the full agonist activity of lipid IV$_A$.** HEK293/hTLR4^{YFP} cells (*a*), HEK293/mTLR4^{YFP} cells (*b*), and MD-2-deficient BMDMs (*c*) were stimulated with LPS·lipid IV$_A$ and MD-2 under serum-free conditions. 1 μg/ml soluble CD14 (*sCD14*) was included for stimulations in MD-2-deficient BMDMs. After overnight stimulation, luciferase activity was measured in HEK293 cell lysates, and mouse tumor necrosis factor α levels were measured in the supernatant of MD-2-deficient BMDMs. The data are reported as the means ± S.D. of three independent wells for each data point. The luciferase activities in *a* and *b* were normalized using *Renilla* luciferase. One representative data set from four replicates is shown in the figure. △, 1 μg/ml LPS; ●, 0.1 μg/ml LPS; ◇, 1 μg/ml lipid IV$_A$; □, 0.1 μg/ml lipid IV$_A$. The MD-2 concentrations used in *a* and *b*, from *left* to *right*, were 5000, 1000, 200, 40, 8, 1.6, 0.32, and 0 ng/ml.

The titration experiments with hMD-2 in HEK293/mTLR4^{YFP} cells (Fig. 1*b*) show that at low concentrations of hMD-2 (<1.6 ng/ml or 53 pM), lipid IV$_A$ did not activate HEK293/mTLR4^{YFP} cells. At higher concentrations of hMD-2 (>40 ng/ml, or 1.3 nM), lipid IV$_A$ activated HEK293/mTLR4^{YFP} cells ~3–4-fold, about half of the response in comparison with

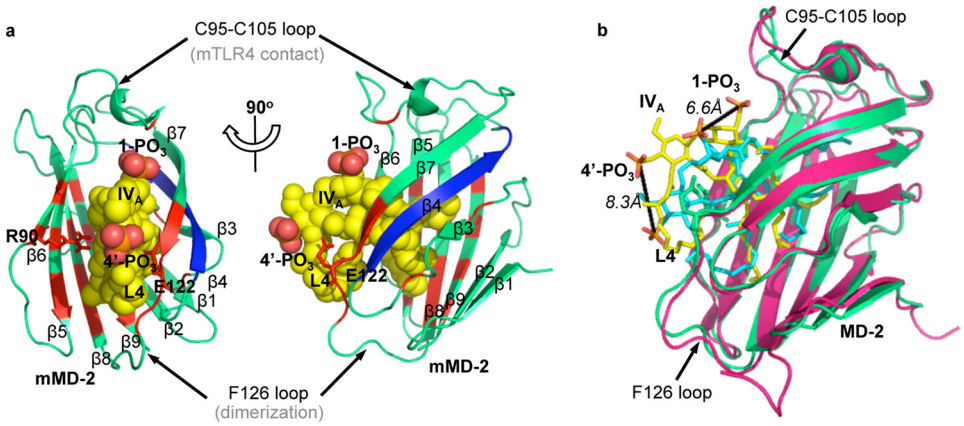

FIGURE 2. **Lipid IV_A packs tilted and shallowly in the mouse MD-2 hydrophobic pocket in the docked mMD-2·lipid IV_A complex.** The docked mMD-2·lipid IV_A complex is shown in two perpendicular views in *a* and overlaid to the hMD-2·lipid IV_A co-crystal structure in *b*. MD-2 is shown in ribbon views in *a* and *b*, and lipid IV_A is shown in sphere view in *a* and stick view in *b*. The residues interacting with lipid IV_A are colored *red*, and the *β4* strand is colored *blue* in *a*. The fourth acyl chain of lipid IV_A is labeled *L4* in both *a* and *b*. *Green*, mMD-2; *yellow*, lipid IV_A in mMD-2; *pink*, hMD-2; *cyan*, lipid IV_A in hMD-2. The graphics were created using PyMol (DeLano Scientific).

LPS stimulation. This indicates that lipid IV_A can function as a partial agonist in HEK293/mTLR4^{YFP} cells and that under the right conditions, both MD-2 and TLR4 seem to be qualitatively dictating the biological responses.

BMDMs from MD-2 Knock-out Mice Required the Presence of Mouse MD-2 to Respond to Lipid IV_A—HEK293/hTLR^{YFP} and HEK293/mTLR^{YFP} cell lines provide a stable environment to quantitatively assess the activity of MD-2. However, these lines are immortalized and genetically engineered; furthermore, they express levels of TLR4 that are higher than true immune cells (supplemental Fig. S3). In addition, HEK293 cells are not professional phagocytes and have a limited profile of inducible proinflammatory cytokines. BMDMs from MD-2 knock-out mice were therefore tested for their responsiveness to lipid IV_A in the presence of purified mMD-2 or hMD-2.

MD-2-null BMDMs responded to LPS stimulation in an hMD-2 dose-dependent manner, which reached a plateau at the hMD-2 concentration of 40 ng/ml (Fig. 1*c*). This concentration likely reflects the amount of MD-2 necessary to saturate TLR4 on the cell surface and to activate intracellular signaling under physiological conditions. Similarly, MD-2-null BMDMs responded to lipid IV_A stimulation in the presence of mMD-2 in a dose-dependent manner until the maximally assessed mMD-2 concentration (Fig. 1*c*) but did not respond to lipid IV_A stimulation when hMD-2 was included regardless of the hMD-2 concentration added (Fig. 1*c*). This indicates that with hMD-2, lipid IV_A does not function as an LPS agonist toward the mouse cells. The partial activation seen in HEK293/mTLR4^{YFP} cells by lipid IV_A at high concentrations of hMD-2 was not observed, which is perhaps a reflection of the physiological levels of mouse TLR4 expression. Thus, both mMD-2 and mTLR4 are required for the species-specific activation of lipid IV_A under physiological conditions.

In summary, it appears that when mouse TLR4 was expressed, the activity of lipid IV_A depended upon the species of MD-2. That is, when mouse TLR4 was matched with mouse MD-2, lipid IV_A was an agonist; when mouse TLR4 was matched with human MD-2, lipid IV_A had no activity (except of at higher levels of mTLR4 in HEK293 cells) and hence functioned as an antagonist. Thus, in the presence of mouse TLR4, the species from which MD-2 was derived determined the character of the response. In contrast, when human TLR4 was expressed, lipid IV_A was not an LPS agonist regardless of the species of MD-2. Hence, both TLR4 and MD-2 appear to be responsible for the species-specific response to lipid IV_A, with the dominance of one over the other depending on the specific combination and expression levels of TLR4·MD-2 examined.

Lipid IV_A Packs Superficially into the Hydrophobic Pocket of Mouse MD-2, with the Diglucosamine Backbone Tilted toward the Cys^{95}–Cys^{105} Loop—Computational docking was performed between lipid IV_A and mMD-2 to understand the essential role of mMD-2 in the species-specific activation of lipid IV_A. Mouse TLR4 was omitted from initial docking because only MD-2, but not TLR4, has been demonstrated to bind LPS or its analogs directly (13). We used the AutoDock docking software, because this approach produces ligand·receptor complexes that closely resemble co-crystal structures (30). In a quality control experiment (supplemental Fig. S4), AutoDock reproduced an hMD-2·lipid IV_A complex highly similar to the co-crystal structure (13), with a root mean square deviation of 0.74 Å and an inhibitory constant (K_i) of 144.85 pM. This K_i is very close to the experimental K_d value between MD-2 and LPS (31).

In the docked lipid IV_A·mMD-2 complex, lipid IV_A packs well into the hydrophobic pocket of mMD-2 (Fig. 2*a*). The acyl chains of lipid IV_A interact extensively with residues lining the hydrophobic pocket, especially residues adjacent to the Phe^{126} loop that has been implicated essential for receptor dimerization (12). The 1,4′-phosphates of lipid IV_A interact weakly with charged residues (*e.g.* Arg^{90} and Glu^{122}) at the pocket entrance (Fig. 2*a*), thus restraining the diglucosamine backbone of lipid IV_A to the pocket entrance. In comparison, none of the *β4* strand residues, which have been suggested to be essential for the species-specific recognition of lipid IV_A (19), are directly involved in lipid IV_A interaction (Fig. 2*a*).

Compared with the hMD-2·lipid IV_A co-crystal structure (13), lipid IV_A packs more superficially in the hydrophobic pocket of mMD-2, with the diglucosamine backbone of lipid IV_A tilted toward the Cys^{95}–Cys^{105} loop (Fig. 2*b*). Consequently, in the docked mMD-2·lipid IV_A complex, the 1-PO_3 and 4′-PO_3 of lipid IV_A are shifted 6.6 and 8.3 Å closer, respectively, to the Cys^{95}–Cys^{105} loop that directly binds mTLR4 (11). In addition, the fourth acyl chain (L4) of lipid IV_A moves toward the surface (Fig. 2*b*) and hence is more exposed to the solvent. The binding kinetics generated by AutoDock between mMD-2 and lipid IV_A was −2.12 kcal mol^{-1} for the expected binding

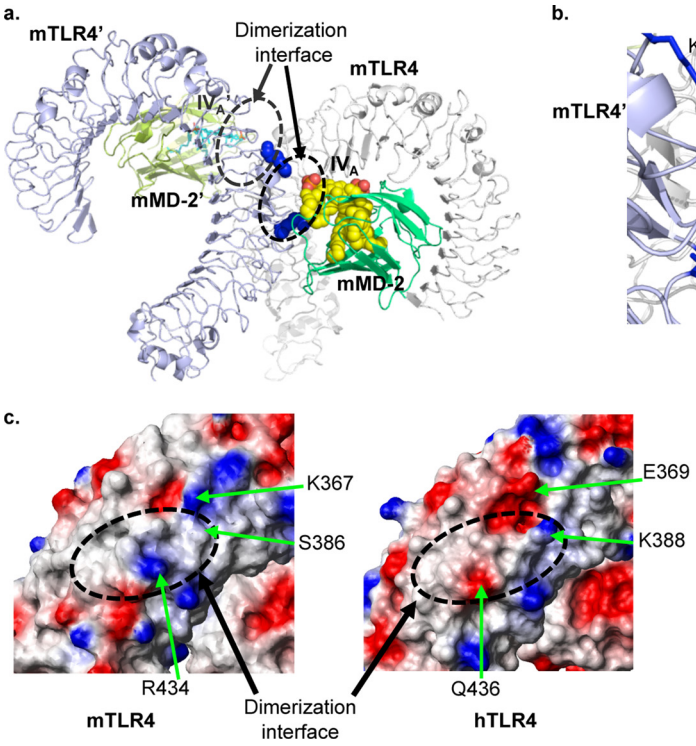

FIGURE 3. **Close proximity is observed between the 4′-PO_3 on lipid IV_A and the positively charged residues on mTLR4 at the dimerization interface.** A dimeric mTLR4·mMD-2·lipid IV_A model is shown in *a*. A zoomed in view of the dimerization interface is shown in *b*. Molecules from the first complex are labeled as mTLR4 (*white ribbon*), mMD-2 (*green ribbon*), and lipid IV_A (*yellow spheres* or *sticks*), and molecules from the second complex are labeled as mTLR4′ (*light purple ribbon*), mMD-2′ (*olive ribbon*), and lipid IV_A′ (*cyan sticks*). The phosphate groups on lipid IV_A are colored *red*. Lys^{367} and Arg^{434} are shown as *blue spheres* in *a* and as *blue sticks* in *b*. The electrostatic surface charges (*c*) of mTLR4 (*left panel*) and hTLR4 (*right panel*) were calculated with MolMol (37). *Red* is for negatively charged surface, *blue* is for positively charged surface, and *white* is for noncharged surface. Residues that differ between mTLR4 and hTLR4 are labeled in *c*. The *dashed circles* in *a* and *c* indicate the dimerization interface.

energy (ΔG_{bin}) and 28.05 mM for the expected inhibitory constant (K_i, 298 K).

The 4′-PO_3 of Lipid IV_A Bound to TLR4·MD-2 Is Adjacent to a Positively Charged Patch on the Opposite mTLR4 at the Dimerization Interface—The coordinates of the mMD-2·lipid IV_A complex were then combined with the crystal structure of mTLR4 to generate an mTLR4·mMD-2·lipid IV_A complex. This complex is very similar to the monomeric hTLR4·hMD-2·LPS complex isolated from the co-crystal structure (see supplemental Fig. S5*a* for the comparison) (12). Except for the opposite orientation of the lipids, the diglucosamine backbone and the two phosphates on the lipids are in very similar positions in the two complexes (supplemental Fig. S5*b*). Thus, the docked mTLR4·mMD-2·lipid IV_A complex is in a favorable conformation to interact with another copy of mTLR4·mMD-2·lipid IV_A complex (denoted as mTLR4′/mMD-2′/lipid IV_A′ from this point on, to differentiate from the original mTLR4·mMD-2·lipid IV_A complex) to form a dimer. Indeed, when the sequences of mTLR4 from the predicted mTLR4·mMD-2·lipid IV_A dimer were superimposed onto the crystal structure of hTLR4 that was defined in the published hTLR4·hMD-2·LPS (see details under "Experimental Procedures"), a dimeric mTLR4·mMD-2·lipid IV_A complex was readily observed (Fig. 3*a*).

Close proximity was observed between the 4′-PO_3 on lipid IV_A and the positively charged residues on mTLR4′ composed of Lys^{367}′ and Arg^{434}′ at the dimerization interface (Fig. 3*b*). The distances between the phosphorous atom on the 4′-PO_3 of lipid IV_A and the nitrogen atoms on Lys^{367}′ and Arg^{434}′ (of mTLR4′) were calculated at 7.2 and 12.4 Å, respectively. These distances are likely to be shortened in the actual, active, and dimeric mTLR4·mMD-2·lipid IV_A complex, because lipid IV_A recognition likely triggers induced fit conformational changes in both mTLR4 and mMD-2 to allow dimerization to occur. These conformational changes likely resemble those observed in the hTLR4·hMD-2·LPS co-crystal structure (12), *i.e.* the extension of the TLR4 solenoid and the folding back of the Phe^{126} loop of MD-2. When present in solution, the 4′-PO_3 on lipid IV_A likely attracts and interacts with the positive patch on mTLR4′ at the dimerization interface to facilitate and enable dimerization and to initiate downstream signaling.

Surface Charge Differences on TLR4 at the Dimerization Interface Account for the Specific Role of TLR4 in the Species-specific Activation of Lipid IV_A—The electrostatic surface charges at the dimerization interface were predicted to be different between mTLR4 and hTLR4 (Fig. 3*c*). Mouse TLR4 has positively charged Lys^{367} and Arg^{434} at the dimerization interface, whereas hTLR4 has the negatively charged Glu^{369} and Gln^{436} at these positions. In addition, the noncharged Ser^{386} in mTLR4 corresponds to a positively charged Lys^{388} in hTLR4. A charge reversal in this area would therefore alter electrostatic forces on the 4′-PO_3 on lipid IV_A, changing the ionic interactions with lipid IV_A at the dimerization interface. We hypothesized that the essential role of TLR4 in the species-specific activation of lipid IV_A arises from different electrostatic surface charges at the dimerization interface.

To examine this possibility, we employed site-directed mutagenesis to engineer single, double, and triple mutants that swap surface charges between mTLR4 and hTLR4. The effects of these mutations were examined by measuring the inducible NF-κB luciferase activity after transient transfection and lipid IV_A stimulation. Mouse MD-2 (at a concentration of 200 ng/ml) was included in all testing conditions, because only mouse MD-2 functions with both hTLR4 and mTLR4.

Compared with the wild type mTLR4 construct, the mTLR4 mutants retained most of their LPS responsiveness (supplemental Fig. S6*a*), indicating that these mutations do not disturb the major structural motif on mTLR4 essential for LPS signaling. Lipid IV_A responsiveness, however, was modified by these

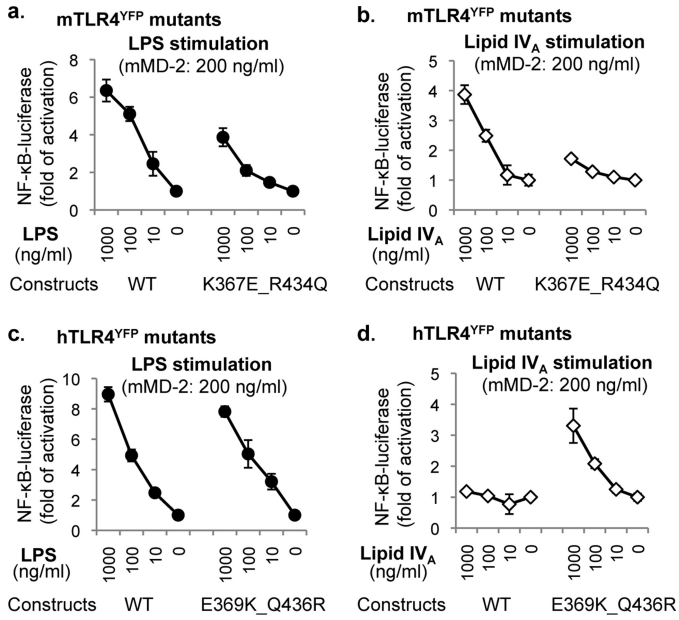

FIGURE 4. **Ionic interactions between lipid IV$_A$ and TLR4 at the dimerization interface are essential for lipid IV$_A$ responsiveness.** HEK293 cells were transiently transfected with: 1) one of the four constructs: mTLR4^{YFP} wild type construct (*WT*), the mTLR4^{YFP} K367E/R434Q mutant (K367E/R434Q), hTLR4^{YFP} wild type construct, and the hTLR4^{YFP} E369K/Q436R mutant (E369K/Q436R); 2) NF-κB luciferase plasmid; and 3) a *Renilla* luciferase plasmid for luciferase assay. After overnight transfection, the cells were stimulated with indicated concentrations of LPS·lipid IV$_A$ and mMD-2 (200 ng/ml) under serum-free conditions. Luciferase activity was measured in cell lysates the next day. The data are reported as the means ± S.D. of three independent wells for each data point. The luciferase activities were normalized from *Renilla* luciferase activity. One representative data set from four replicates is shown in the figure.

mutations. As the dimerization interface become less positively charged, the lipid IV$_A$ responsiveness decreased (supplemental Fig. S6*b*), with the most profound effect on the double mutant K367E/R434Q (Fig. 4, *a* and *b*). Thus, ionic interactions between the 4′-PO$_3$ of lipid IV$_A$ and the positive patch on mTLR4 at the dimerization interface appeared to be required for lipid IV$_A$ activation.

Conversely, all of the hTLR4 mutants retained their LPS responsiveness (supplemental Fig. S7*a*). However, the engraftment of the positively charged residues from the dimerization interface of mouse TLR4 to its human counterpart had a dramatic effect on lipid IV$_A$ signaling (supplemental Fig. S7*b*). Enhanced responses to lipid IV$_A$ were weakly detected in the single mutants E369K and Q436R but were more profoundly observed in the double mutant E369K/Q436R (Fig. 4, *c* and *d*) and the triple mutant E369K/K388S/Q436R (supplemental Fig. S7*b*). In other words, the gain of positive charge at the dimerization interface alone on hTLR4 is sufficient to convert the mMD-2·hTLR4 complex from a lipid IV$_A$ nonresponder to a lipid IV$_A$ responder. Thus, mMD-2-mediated ionic interactions between the 4′-PO$_3$ on lipid IV$_A$ and the positive patch on TLR4 (wild type mTLR4 the hTLR4 double mutant E369K/Q436R) are essential for the LPS mimetic activity of lipid IV$_A$.

DISCUSSION

Several studies have been dedicated to study the underlying mechanism for the species-specific recognition of lipid IV$_A$, because it has long been clear that understanding this pharmacology would offer important insights for how the LPS receptor functions. Surprisingly, these studies have achieved contradictory results. Although we (16) and Beutler and co-workers (17) suggested that TLR4 is responsible for the species-specific activation of lipid IV$_A$, Miller and co-workers (18) and Miyake and co-workers (14) indicated that MD-2 is responsible for this species specificity. In all of these experiments, the animal serum that included variable amounts of bovine MD-2 was included in the assays, which added a confounding variable. In addition, transient transfection was generally used to introduce TLR4 and MD-2 into cells, and therefore, adequate expressions of TLR4 and MD-2 were often assumed. This was especially the case for mouse MD-2, which in our hands was minimally expressed after transfection in any mammalian cell line. Miyake and co-workers (14) appear to have had similar problems. Their report focusing on the species-specific response to lipid IV$_A$ revealed that they were unable to observe any response, regardless of the ligand, when mouse MD-2 was transfected with human TLR4 (14). One important advance here is that we were able to provide recombinant protein as the source of MD-2 at defined concentrations. Hence, an important combination of TLR4·MD-2 can now be tested (mouse MD-2 plus human TLR4). We found that mTLR4 is a prerequisite but not the sole determinant for the agonist activity of lipid IV$_A$, which also required the presence of mMD-2. The dual requirement of mTLR4 and mMD-2 for the agonistic activity of lipid IV$_A$ was also confirmed in MD-2-deficient BMDMs, a relevant system in which levels of mTLR4 are physiologic.

We then used computational docking and modeling to generate a working model for lipid IV$_A$ activation. It appears that both mMD-2 and mTLR4 are required for lipid IV$_A$ signaling, because only the mMD-2·mTLR4 complex provides an environment for lipid IV$_A$ to efficiently interact with mTLR4′ at the dimerization interface. The essential role of mTLR4 arises mainly from its unique surface charge at the dimerization interface (Lys^{367} and Arg^{434}) and, hence, its capability to interact with the 4′-PO$_3$ of lipid IV$_A$ through ionic interactions.

In comparison, the essential role of mMD-2 arises from its ability to bind lipid IV$_A$ so that the ligand sits shallowly in its hydrophobic pocket in a tilted conformation. This provides the proper scaffold for the 4′phosphate of lipid IV$_A$ to interact with a positively charged patch on mouse TLR4 at the dimerization interface and trigger receptor activation. This unique scaffolding role of mMD-2 in packaging the tetra-acylated lipid IV$_A$ derives from differences in its hydrophobic pocket in comparison with hMD-2. The hydrophobic pockets of hMD-2 and mMD-2 differ in their fine volume, dimension, and adjacent surface charges (supplemental Fig. S8). Although the hydrophobic pocket of hMD-2 looks like a true pocket, *i.e.* a deep invagination with a sealed bottom, the hydrophobic pocket of mMD-2 is more likely a funnel structure (supplemental Fig. S8*a*). Its pocket is wider and shallower near the entrance but deeper at the bottom, rendering the appearance of a "hole" at the bottom. The surface charges near the pocket entrance are also slightly different between the two species of MD-2. Human MD-2 has the strongly positively charged Lys^{122} on the β7 strand that flanks the pocket entrance and Lys^{125} on the Phe^{126}

loop that mediates dimerization (12). In comparison, mMD-2 has a negatively charged Glu^{122} at the pocket entrance and the highly hydrophobic Leu^{125} on the Phe^{126} loop. The charge reversal from Lys^{122} to Glu^{122} likely introduces repulsive forces toward the bis-phosphate diglucosamine backbone of lipid IV_A, whereas a gain of hydrophobicity from Lys^{125} to Leu^{125} in mMD-2 likely facilitates interaction with the acyl chains of lipid IV_A. Consequently, we predict that lipid IV_A packs more superficially in the mMD-2 hydrophobic pocket than in the human receptor, with the diglucosamine backbone tilted toward the Cys^{95}–Cys^{105} loop (which binds MD-2 to TLR4). Supporting data for this prediction have been reported by Muroi and Tanamoto (32), who demonstrated that when Glu^{122} was mutated to Lys^{122} on mMD-2, lipid IV_A no longer functioned as an agonist. In a sense, it is the hydrophobic pocket of mMD-2 that determines the species-specific pharmacology of lipid IV_A with respect to mMD-2.

In the published hTLR4·hMD-2·LPS co-crystal structure (12), extensive hydrophobic interactions were observed at the dimerization interface, involving hydrophobic residues Phe^{126}, Ile^{124}, Leu^{87}, Met^{85}, and Val^{82} on hMD-2, the sixth acyl chain of LPS, and hydrophobic residues $Phe^{440\prime}$, $Leu^{444\prime}$, and $Phe^{463\prime}$ on the opposing hTLR4′. When Phe^{126} on hMD-2 was mutated to alanine, receptor dimerization did not occur (11). Hence, the authors proposed that hydrophobic interactions are the primary driving force for receptor dimerization and activation (11, 12). This hypothesis was supported by mutagenesis studies from Jerala and co-workers (33), showing that when the hydrophobic residues at the dimerization interface on MD-2 and TLR4 were mutated to Ala, receptor activation was not observed. Therefore, hydrophobic interactions at the dimerization interface appeared to be the driving force for receptor dimerization. These mutagenesis data on MD-2 and TLR4, however, should not be confused with "mutagenesis on LPS." These data only demonstrated that hydrophobic interactions arising from hydrophobic residues on MD-2 and TLR4 are essential for receptor dimerization. They did not suggest that hydrophobic interactions derived from the sixth acyl chain of LPS at the dimerization interface are essential for receptor activation. In fact, the Phe^{126} loop on hMD-2 has to "fold back" to accommodate the extra acyl chain of LPS at the dimerization interface to allow dimerization to occur (11, 12), strongly suggesting a redundancy of hydrophobic interactions at the dimerization interface in regard to receptor dimerization.

It should be noted that the present study does not contradict these findings. Except residue 85 which is a Met in hMD-2, but an Ile in mMD-2, all of the hydrophobic residues on MD-2 and TLR4′ at the dimerization interface are completely conserved between the two species. Therefore, hydrophobic interactions between mMD-2 and mTLR4′ are preserved at the dimerization interface, which can still function as the primary driving force for receptor dimerization. These interactions by themselves, however, are not sufficient to provide enough forces for receptor dimerization. Additional forces such as ionic interactions, as described here, are required for the formation of an active receptor complex. Although the sixth acyl chain of *E. coli* lipid A may enhance receptor activation, it should be noted that penta-acylated lipid A is capable of activating TLR4·MD-2 with the same potency as hexa-acylated lipid A (34). Thus, whereas hydrophobic forces are clearly critical for TLR4·MD-2 activation, they are not sufficient.

A noticeable difference between the hTLR4·hMD-2·LPS crystal structure and our lipid IV_A activation model is the opposite orientation of the lipids in the MD-2 hydrophobic pockets. This difference should not result in a significant functional difference, because lipid IV_A can be considered as functionally symmetric. Additionally, it is plausible that lipid A inserts into MD-2 in both orientations and that only one orientation was well resolved by crystallographic approaches. This might happen if a particular crystal was analyzed in which one orientation predominated or even if there were a preponderance of one orientation over the other. It is also possible that the current configuration of LPS is favored in the co-crystal structure, because the co-crystallized LPS has an asymmetric core polysaccharide that interacts extensively with TLR4 (12).

Lipid IV_A has partial activity in the equine TLR4·MD-2 receptor (19). One explanation for this observation is that the relative orientation between equine MD-2 and equine TLR4 are different from other species. In particular, repulsive forces from the phosphate of lipid IV_A combined with residue 122 on MD-2 may not be required to "lift" lipid IV_A up in the horse receptor, accounting for the partial activity. Similar to human MD-2, equine MD-2 has a positively charged residue, Arg^{122}, at the hydrophobic pocket entrance. Therefore, repulsive forces cannot be generated at the pocket entrance to lift MD-2 up. However, in a recent separate study, we identified that not only residues near the hydrophobic pocket of MD-2 are essential for lipid IV_A activation but also residues at the A patch (11, 12) of MD-2 that physically associate with TLR4 are important for lipid IV_A activation. Specifically, we identified that Gly^{69} and Tyr^{42} on mMD-2 are required for a full response to lipid IV_A.[5] Because Gly^{69} and Tyr^{42} reside at the opposite surface of the dimerization interface, these residues likely indirectly affect receptor dimerization through affecting the MD-2·TLR4 binding angle. Because equine MD-2 has Ser^{42} instead of Tyr^{42}, the binding angle between equine MD-2 and equine TLR4 could be slightly different from the human and mouse complexes. Hence, lipid IV_A functions as a partial agonist for the equine receptor.

Despite of all its implications, the resolution of the complete TLR4·MD-2/LPS crystal structure did not identify the charge interactions on TLR4 at the dimerization interface that appear to be so important for lipid A activity. In other words, the crystal structure of TLR4·MD-2/LPS did not allow us to make conclusions concerning whether the physical proximity between the charged groups of LPS and hTLR4 play a functional role in LPS activation. As can be seen here, the use of lipid IV_A as a selective lipid A agonist allows us to address questions concerning the meaning of the receptor structure that might otherwise be difficult to test. Because both MD-2 and TLR4 are required for lipid IV_A signaling, we were able to dissect the roles of TLR4 and MD-2 on receptor activation to identify a key ionic interaction that might otherwise have been missed.

[5] J. Meng, J. R. Drolet, B. Monks, and D. T. Golenbock, unpublished data.

Indeed, a practical application of the results presented here are opportunities for designing better adjuvants. New compounds with alterations in charge and the way in which they bind to MD-2 (via acylation patterns and/or chain length) are likely to affect immunogenicity differentially, and the effects of alterations in lipid A structure should be amenable to prediction using an approach similar to that presented here. The view that minor alterations in adjuvants can have major effects on outcomes has been borne out by recent clinical trials for important new vaccines, such as the circumsporozoite vaccine for malaria (35, 36).

Acknowledgments—We thank Kristen Halmen for help on bone marrow-derived macrophages preparation, Brian Monks for help on mutagenesis, and Rosane DeOliveira for help with flow cytometry. We thank Dr. C. James McKnight for critical reading of this manuscript.

REFERENCES

1. Janeway, C. A., Jr., and Medzhitov, R. (1998) *Semin. Immunol.* **10,** 349–350
2. Rangel-Frausto, M. S. (2005) *Arch. Med. Res.* **36,** 672–681
3. Angus, D. C., Linde-Zwirble, W. T., Lidicker, J., Clermont, G., Carcillo, J., and Pinsky, M. R. (2001) *Crit. Care Med.* **29,** 1303–1310
4. Qureshi, N., Takayama, K., and Ribi, E. (1982) *J. Biol. Chem.* **257,** 11808–11815
5. Homma, J. Y., Matsuura, M., and Kumazawa, Y. (1990) *Adv. Exp. Med. Biol.* **256,** 101–119
6. Takada, H., and Kotani, S. (1989) *Crit. Rev. Microbiol.* **16,** 477–523
7. Fujimoto, Y., Adachi, Y., Akamatsu, M., Fukase, Y., Kataoka, M., Suda, Y., Fukase, K., and Kusumoto, S. (2005) *J. Endotoxin Res.* **11,** 341–347
8. Montminy, S. W., Khan, N., McGrath, S., Walkowicz, M. J., Sharp, F., Conlon, J. E., Fukase, K., Kusumoto, S., Sweet, C., Miyake, K., Akira, S., Cotter, R. J., Goguen, J. D., and Lien, E. (2006) *Nat. Immunol.* **7,** 1066–1073
9. Raetz, C. R., Reynolds, C. M., Trent, M. S., and Bishop, R. E. (2007) *Annu. Rev. Biochem.* **76,** 295–329
10. Golenbock, D. T., Hampton, R. Y., Qureshi, N., Takayama, K., and Raetz, C. R. (1991) *J. Biol. Chem.* **266,** 19490–19498
11. Kim, H. M., Park, B. S., Kim, J. I., Kim, S. E., Lee, J., Oh, S. C., Enkhbayar, P., Matsushima, N., Lee, H., Yoo, O. J., and Lee, J. O. (2007) *Cell* **130,** 906–917
12. Park, B. S., Song, D. H., Kim, H. M., Choi, B. S., Lee, H., and Lee, J. O. (2009) *Nature*
13. Ohto, U., Fukase, K., Miyake, K., and Satow, Y. (2007) *Science* **316,** 1632–1634
14. Akashi, S., Nagai, Y., Ogata, H., Oikawa, M., Fukase, K., Kusumoto, S., Kawasaki, K., Nishijima, M., Hayashi, S., Kimoto, M., and Miyake, K. (2001) *Int. Immunol.* **13,** 1595–1599
15. Schromm, A. B., Lien, E., Henneke, P., Chow, J. C., Yoshimura, A., Heine, H., Latz, E., Monks, B. G., Schwartz, D. A., Miyake, K., and Golenbock, D. T. (2001) *J. Exp. Med.* **194,** 79–88
16. Lien, E., Means, T. K., Heine, H., Yoshimura, A., Kusumoto, S., Fukase, K., Fenton, M. J., Oikawa, M., Qureshi, N., Monks, B., Finberg, R. W., Ingalls, R. R., and Golenbock, D. T. (2000) *J. Clin. Invest.* **105,** 497–504
17. Poltorak, A., Ricciardi-Castagnoli, P., Citterio, S., and Beutler, B. (2000) *Proc. Natl. Acad. Sci. U.S.A.* **97,** 2163–2167
18. Hajjar, A. M., Ernst, R. K., Tsai, J. H., Wilson, C. B., and Miller, S. I. (2002) *Nat. Immunol.* **3,** 354–359
19. Walsh, C., Gangloff, M., Monie, T., Smyth, T., Wei, B., McKinley, T. J., Maskell, D., Gay, N., and Bryant, C. (2008) *J. Immunol.* **181,** 1245–1254
20. Edelhoch, H. (1967) *Biochemistry* **6,** 1948–1954
21. Latz, E., Visintin, A., Lien, E., Fitzgerald, K. A., Monks, B. G., Kurt-Jones, E. A., Golenbock, D. T., and Espevik, T. (2002) *J. Biol. Chem.* **277,** 47834–47843
22. Liu, W. C., Oikawa, M., Fukase, K., Suda, Y., and Kusumoto, S. (1999) *Bull. Chem. Soc. Jpn.* **72,** 1377–1385
23. Hirschfeld, M., Ma, Y., Weis, J. H., Vogel, S. N., and Weis, J. J. (2000) *J. Immunol.* **165,** 618–622
24. Fitzgerald, K. A., Palsson-McDermott, E. M., Bowie, A. G., Jefferies, C. A., Mansell, A. S., Brady, G., Brint, E., Dunne, A., Gray, P., Harte, M. T., McMurray, D., Smith, D. E., Sims, J. E., Bird, T. A., and O'Neill, L. A. (2001) *Nature* **413,** 78–83
25. Nagai, Y., Akashi, S., Nagafuku, M., Ogata, M., Iwakura, Y., Akira, S., Kitamura, T., Kosugi, A., Kimoto, M., and Miyake, K. (2002) *Nat. Immunol.* **3,** 667–672
26. Meng, J., Parroche, P., Golenbock, D. T., and McKnight, C. J. (2008) *J. Biol. Chem.* **283,** 3376–3384
27. Huey, R., Morris, G. M., Olson, A. J., and Goodsell, D. S. (2007) *J. Comput. Chem.* **28,** 1145–1152
28. Morris, G. M., Goodsell, D. S., Halliday, R. S., Huey, R., Hart, W. E., Belew, R. K., and Olson, A. J. (1998) *J. Comput. Chem.* **19,** 1639–1662
29. Sanner, M. F. (1999) *J. Mol. Graph Model* **17,** 57–61
30. Moitessier, N., Henry, C., Maigret, B., and Chapleur, Y. (2004) *J. Med. Chem.* **47,** 4178–4187
31. Prohinar, P., Re, F., Widstrom, R., Zhang, D., Teghanemt, A., Weiss, J. P., and Gioannini, T. L. (2007) *J. Biol. Chem.* **282,** 1010–1017
32. Muroi, M., and Tanamoto, K. (2006) *J. Biol. Chem.* **281,** 5484–5491
33. Resman, N., Vasl, J., Oblak, A., Pristovsek, P., Gioannini, T. L., Weiss, J. P., and Jerala, R. (2009) *J. Biol. Chem.* **284,** 15052–15060
34. Rietschel, E. T., Brade, L., Schade, U., Galanos, C., Freudenberg, M., Lüderitz, O., Kusumoto, S., and Shiba, T. (1987) *Eur. J. Biochem.* **169,** 27–31
35. Bejon, P., Lusingu, J., Olotu, A., Leach, A., Lievens, M., Vekemans, J., Mshamu, S., Lang, T., Gould, J., Dubois, M. C., Demoitié, M. A., Stallaert, J. F., Vansadia, P., Carter, T., Njuguna, P., Awuondo, K. O., Malabeja, A., Abdul, O., Gesase, S., Mturi, N., Drakeley, C. J., Savarese, B., Villafana, T., Ballou, W. R., Cohen, J., Riley, E. M., Lemnge, M. M., Marsh, K., and von Seidlein, L. (2008) *N. Engl. J. Med.* **359,** 2521–2532
36. Abdulla, S., Oberholzer, R., Juma, O., Kubhoja, S., Machera, F., Membi, C., Omari, S., Urassa, A., Mshinda, H., Jumanne, A., Salim, N., Shomari, M., Aebi, T., Schellenberg, D. M., Carter, T., Villafana, T., Demoitié, M. A., Dubois, M. C., Leach, A., Lievens, M., Vekemans, J., Cohen, J., Ballou, W. R., and Tanner, M. (2008) *N. Engl. J. Med.* **359,** 2533–2544
37. Koradi, R., Billeter, M., and Wuthrich, K. (1996) *J. Mol. Graph* **14,** 51–55, 29–32